Dark matter scatterings in space and underground direct detections

Yu-Feng Zhou

Institute of Theoretical Physics
Chinese Academy of Sciences

Yan-Hao Xu, Chen Xia, YFZ,
arXiv:2111.05559 (JCAP), arXiv:2206.11454 (PRD)
Mai Qiao, Chen Xia, YFZ , arXiv:2307.xxxx

2023-07-02，李学潜老师80华诞

Why dark matter is a problem for particle physics ?

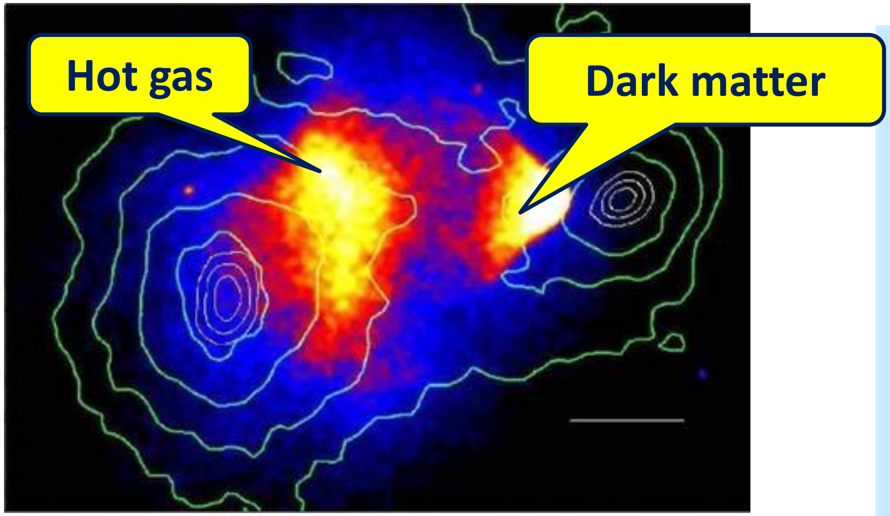

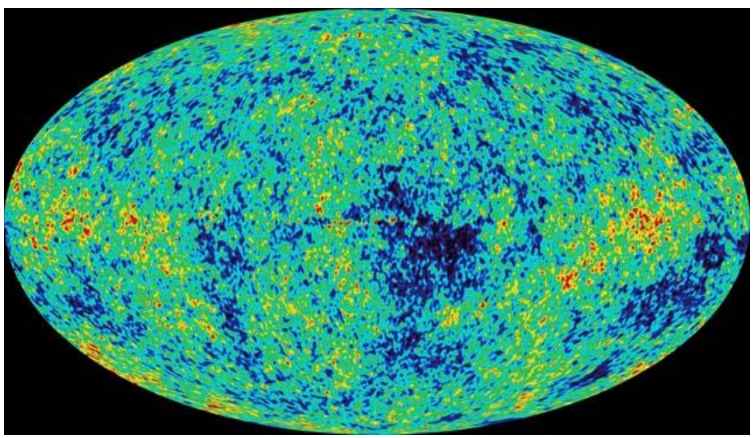

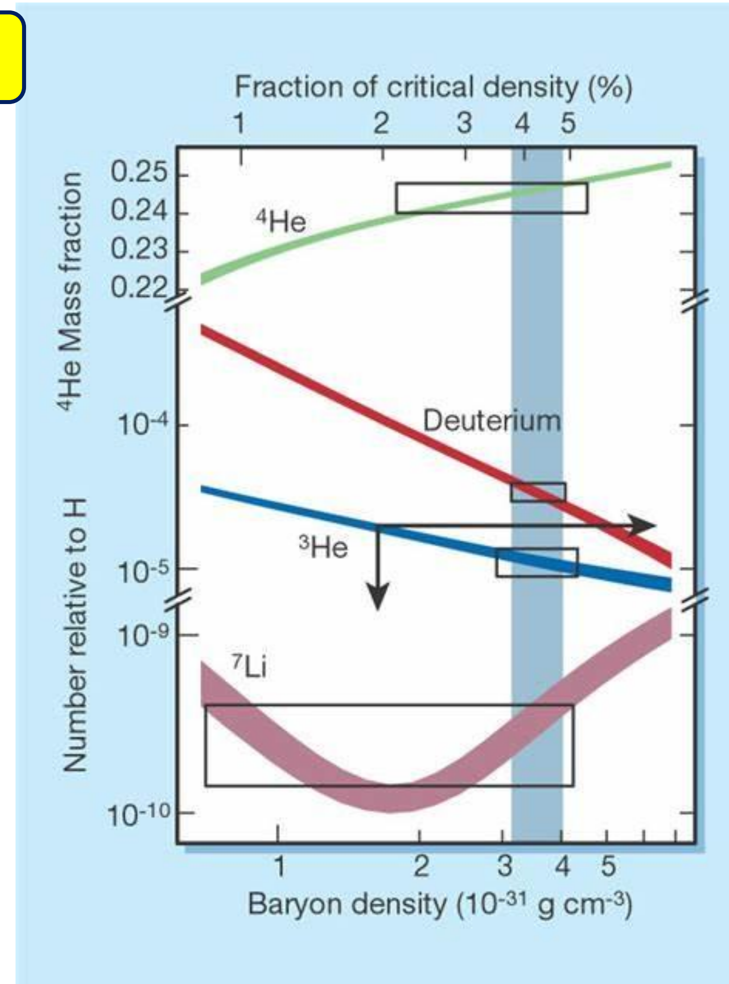

$$\Omega_{DM}h^2 = 0.1123 \pm 0.0035; \Omega_b h^2 = 0.02260 \pm 0.00053$$

How to detect dark matter ?

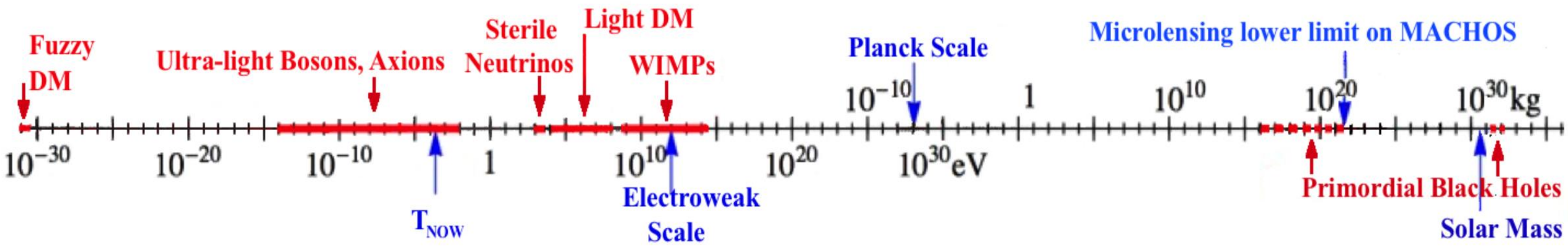

Collider search vs. Direct detection

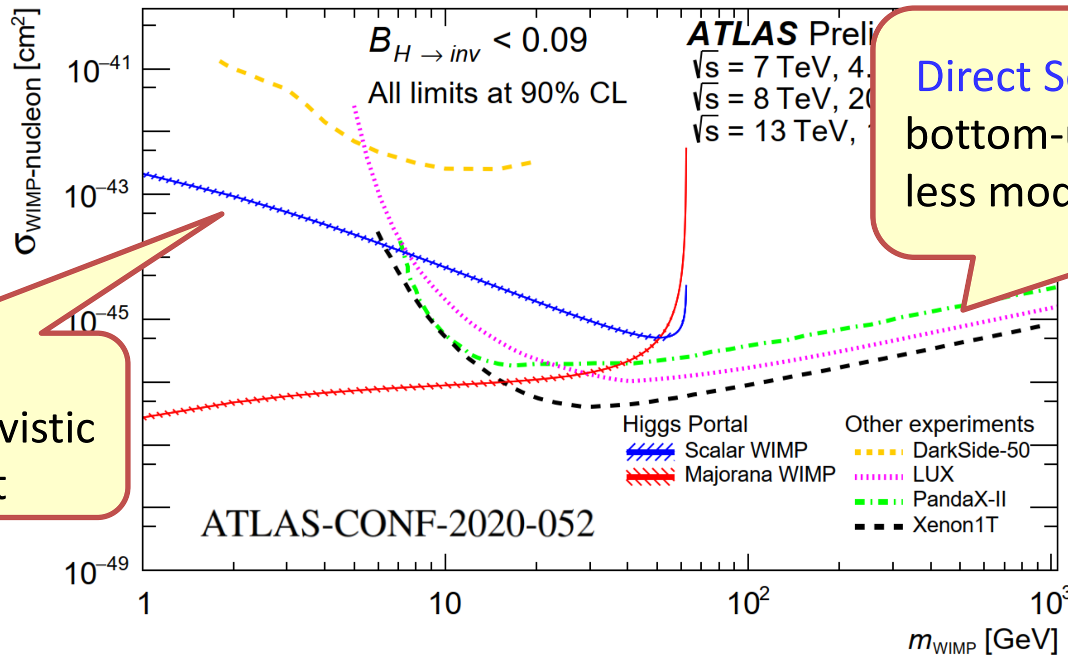

Direct Searches
bottom-up, nonrelativistic
less model-dependent

Collider Searches
top-down， relativistic
model dependent

The search for particle DM in a vast parameter space requires complementary approaches

Frontiers in DM direct searches

The ceiling

larger cross section
$\sigma > 10^{-30}$ cm^2

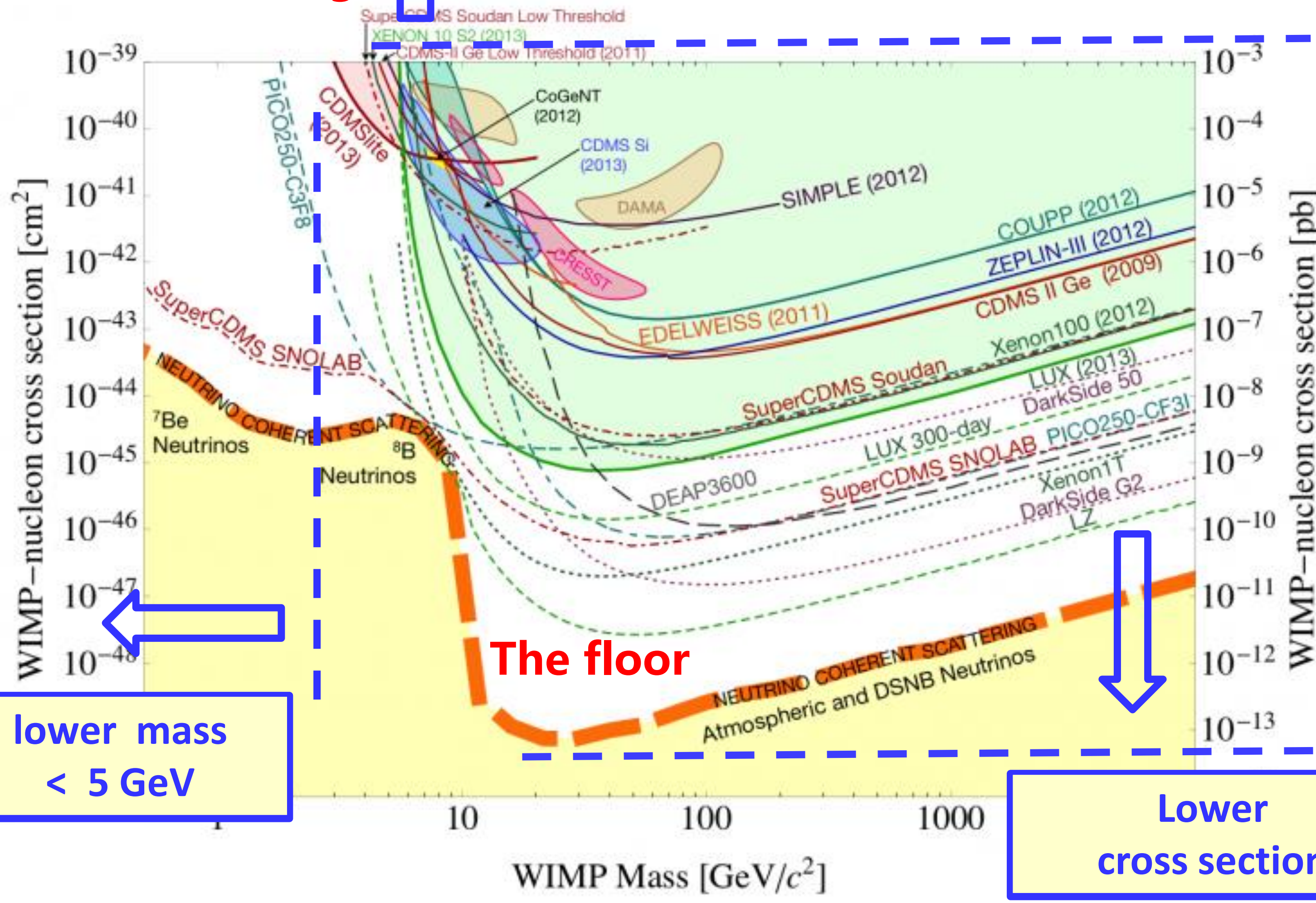

The floor

lower mass
< 5 GeV

Lower
cross section

DM scattering in space: CMB

DM-proton scattering 380000 yrs after the Big Bang

- ❑ Distortion of CMB spectrum
- ❑ Suppression of small sale structure (drag force)

Constraints: $\sigma < 10^{-27}\,\mathrm{cm}^2$ @ 1 keV

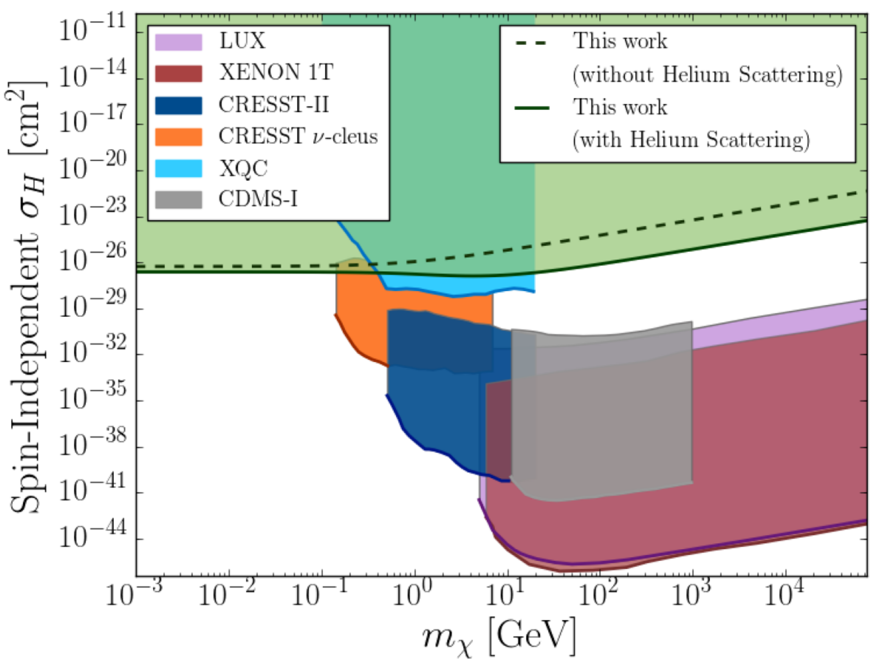

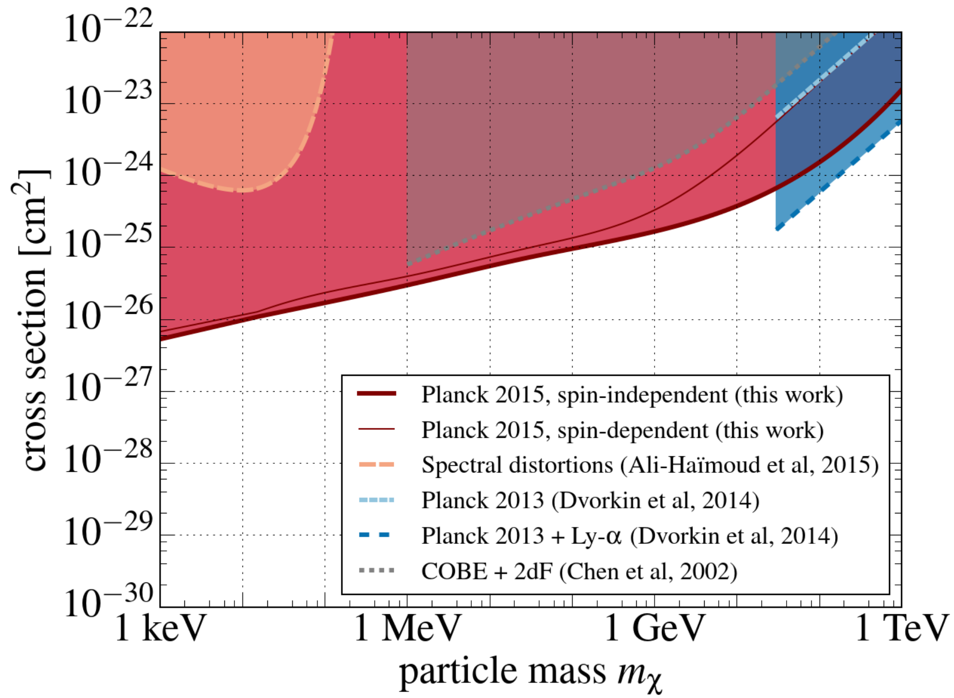

Constraints insensitive to DM particle mass

Gluscevic & Boddy, arXiv:1712.07133

DM scattering in space: structure formation

DM-proton scattering damp structure perturbation
Distribution of dwarf satellite galaxies is modified
$\sigma < 6 \times 10^{-30}$ cm^2 @ 10 keV, ($< 10^{-27}$ cm^2 @ 10 GeV)
Upper limits scale with DM mass as $m^{1/4}$ for m <<1 GeV

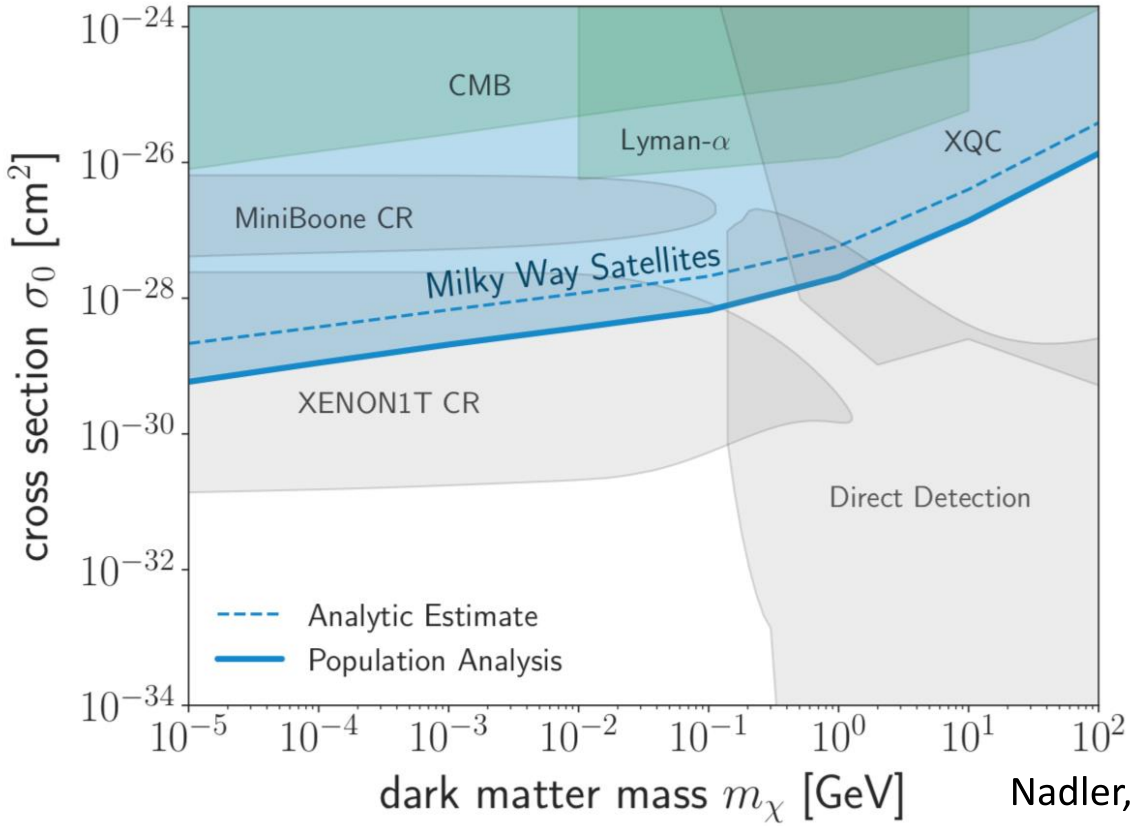

Nadler, et al., arXiv:1904.10000
DES, arXiv:2008.00022

Constraints insensitive to DM particle mass

DM scattering in space: gas cooling

DM above KeV has a temperature higher than the coldest atomic gas

$$T_x \sim m_x v_x^2 \simeq 10^4 \text{ K} \left(\frac{m_x}{\text{MeV}}\right)\left(\frac{v_x}{10^{-3}}\right)^2,$$

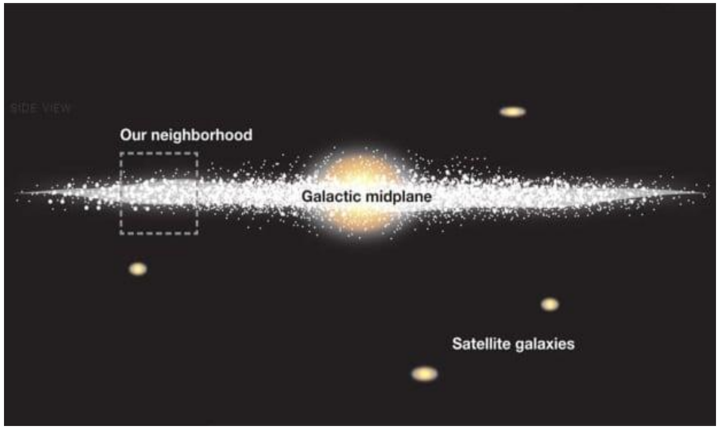

dwarf galaxies

DM-proton scattering heat the gas and change its cooling rate

$\sigma < 10^{-(23\text{-}25)}\,\text{cm}^2$ for a large mass range

10^{-23} eV -- 10^{-10} eV from dwarf galaxy Leo T

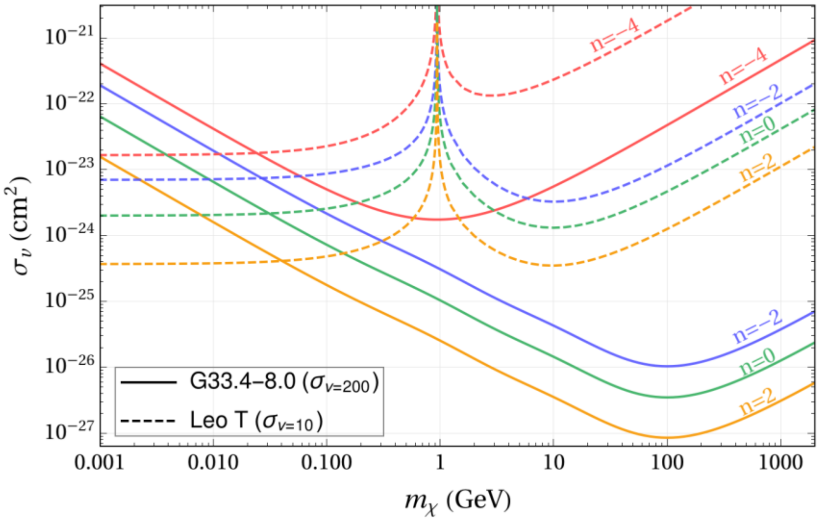

Wadeker & Farrar, arXiv:1903.12190

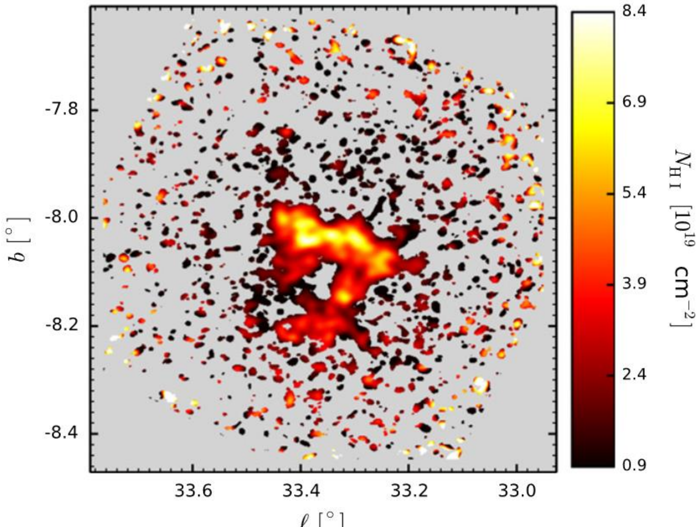

Gas cloud G33.4-8.0

DM flux has a preferred direction in the Earth frame

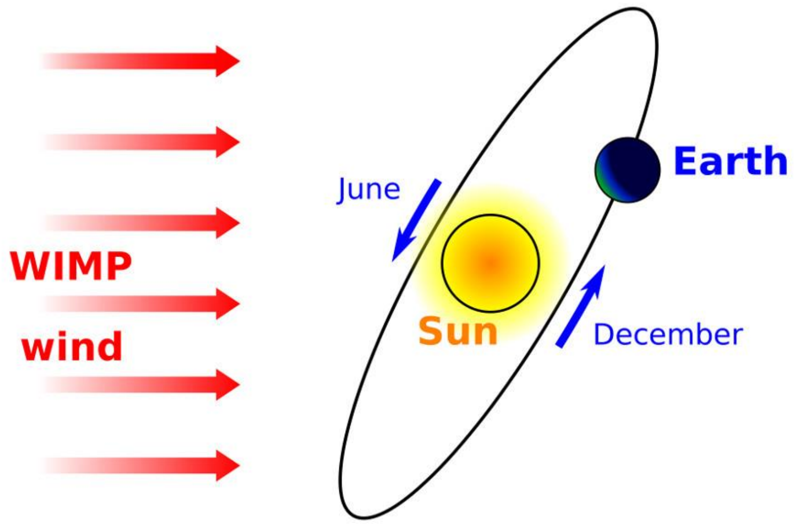

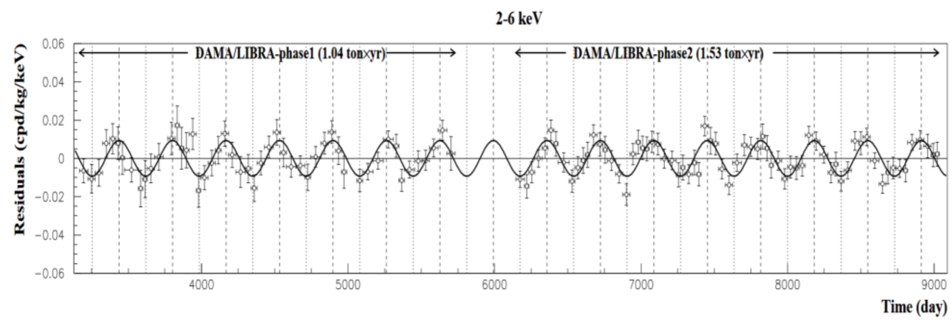

DAMA: arXiv:2209.00882

Standard halo model

$$f_{\rm halo}(\boldsymbol{v}) = \frac{n_0}{N} \exp\left(-\frac{\boldsymbol{v}^2}{v_0^2}\right) \Theta(v_{\rm esc} - |\boldsymbol{v}|),$$

Advantages for DM search

- ❑ reject all isotropic backgrounds
- ❑ go beyond the neutrino floor
- ❑ uniquely identify DM

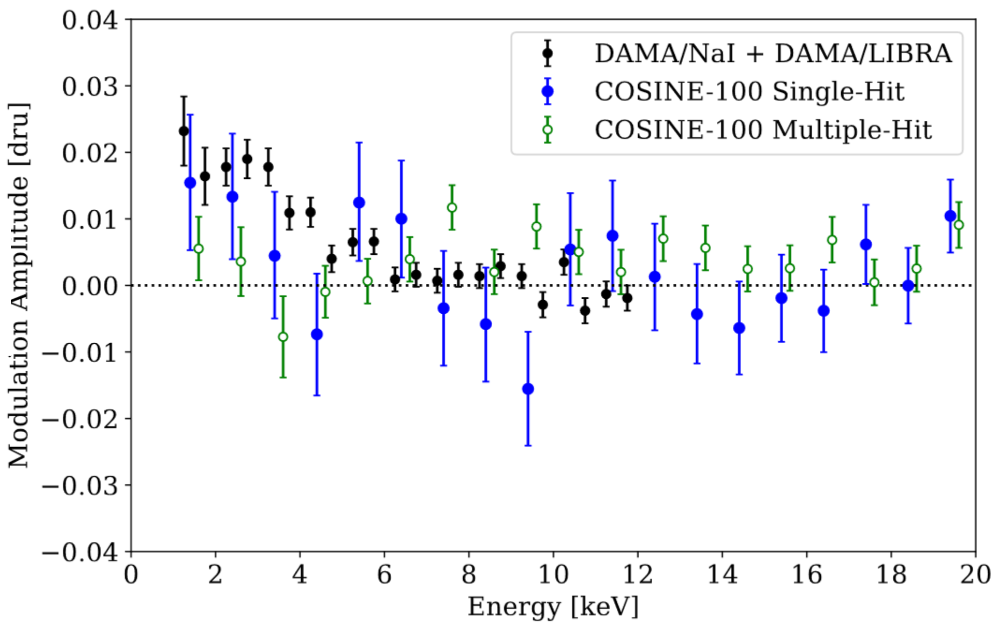

COSINE: arXiv:2111.08863

Directional search with lower thresholds

Borexino : Scintillator + Cherenkov light
Detection of sub-MeV ^{7}Be solar neutrino (0.6—0.8 MeV)

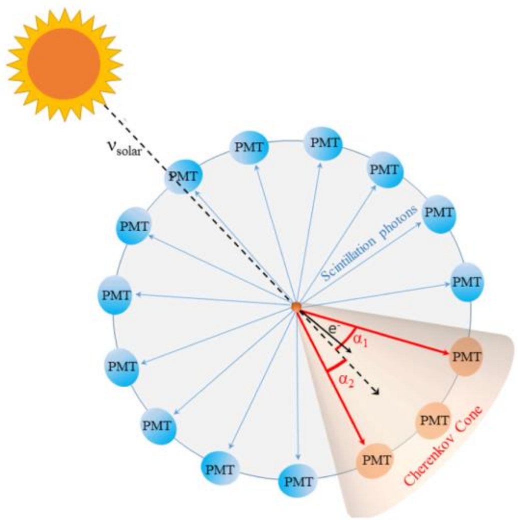

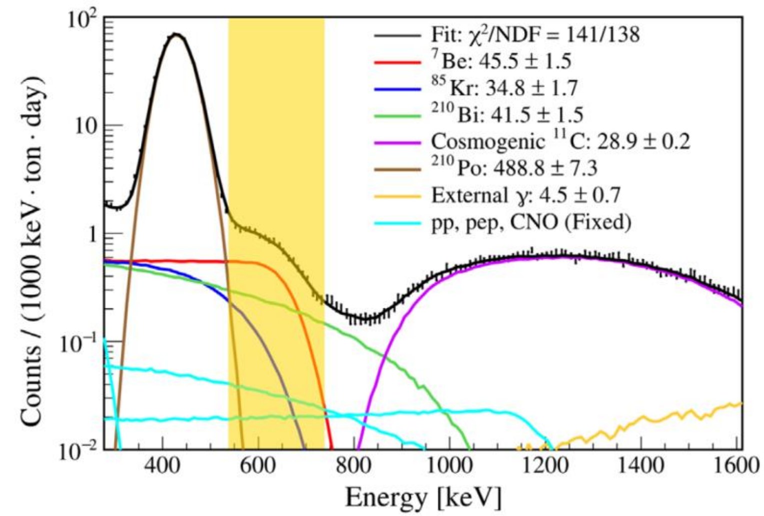

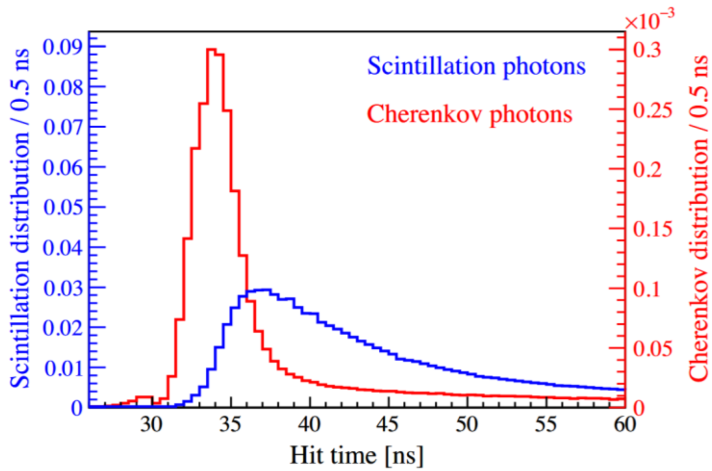

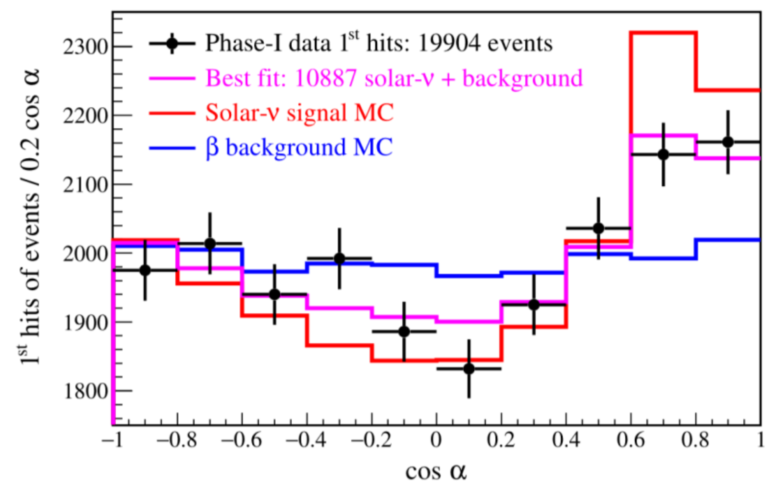

Borexino, PhysRevLett.128.091803(2022)

Beyond the solar neutrino floor

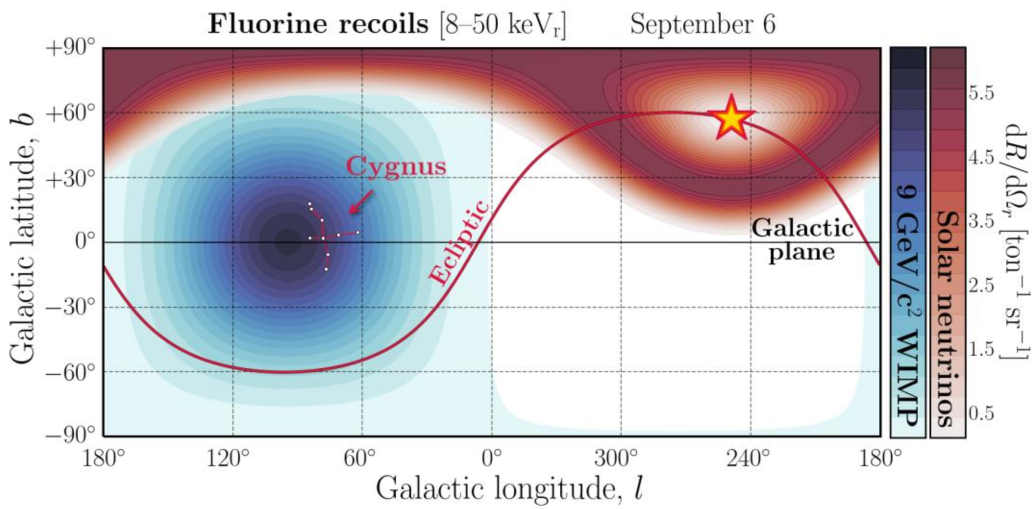

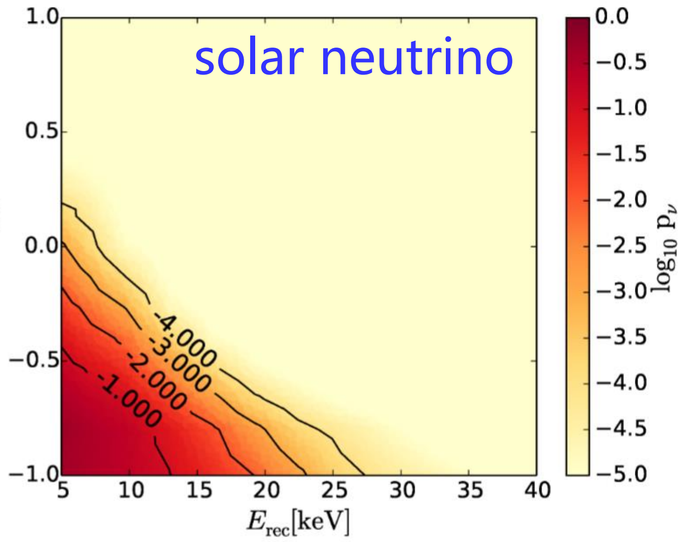

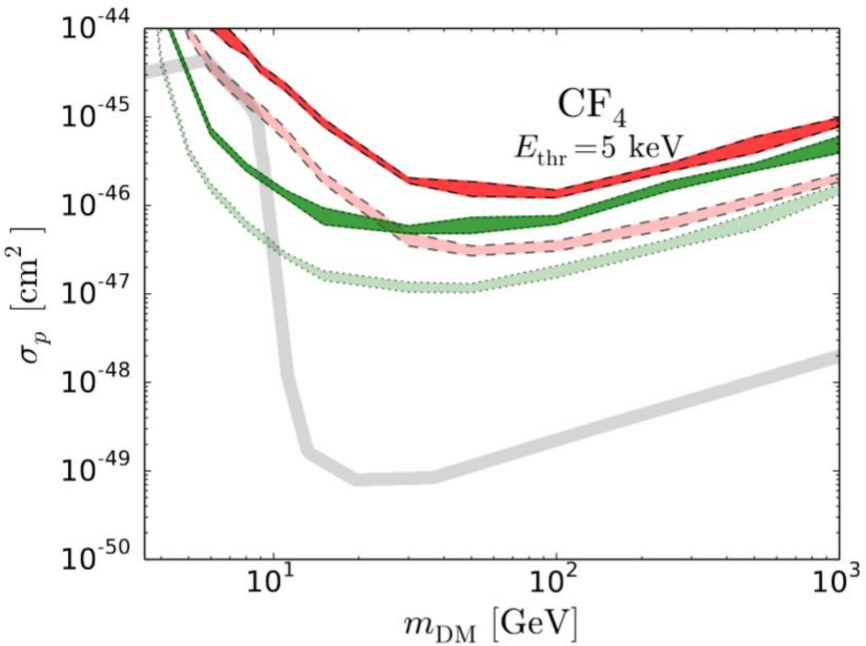

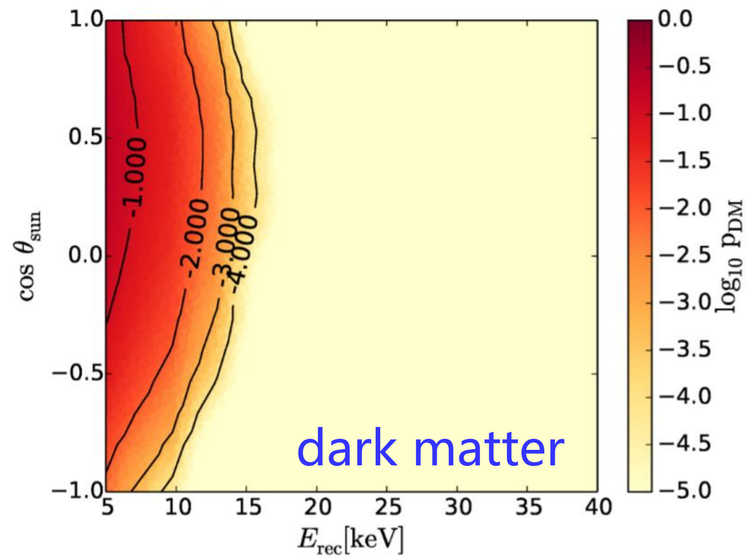

P. Grothaus, et al, arXiv:1406.5047

Methods for directional searches

Direct approaches

- Gas TPCs: CYGNUS, DMPTC m³ (e.g. CF_4)
- Nuclear Emulsions: NEWSdm (AgBr)
- Crystal defects (Nitrogen vacancy in diamond)
- 2d materials
- DNA strands

Indirect approaches

- Anisotropic scintillators ($Z_n W O_4$)
- Columnar Recombination

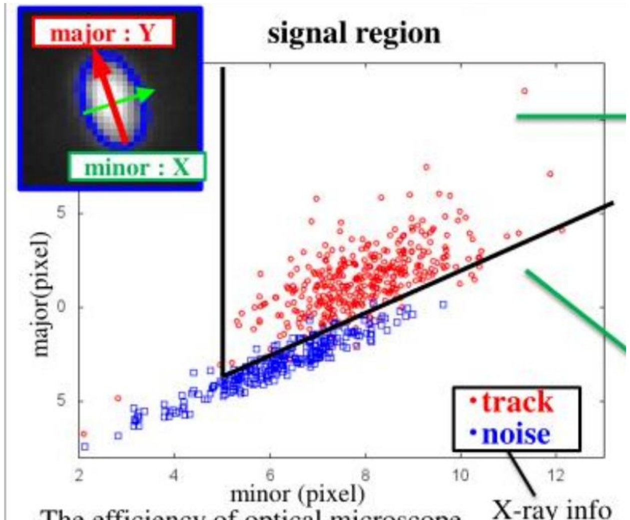

The efficiency of optical microscope is measured with comparing both optical and X-ray event data.

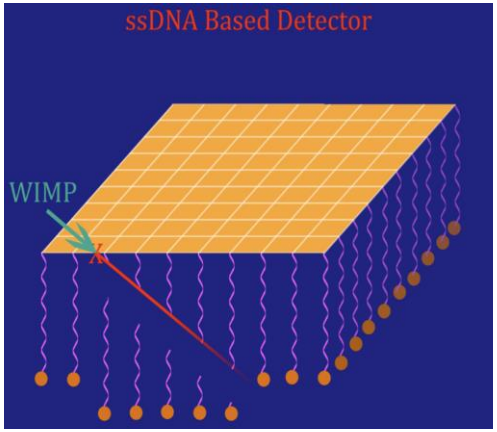

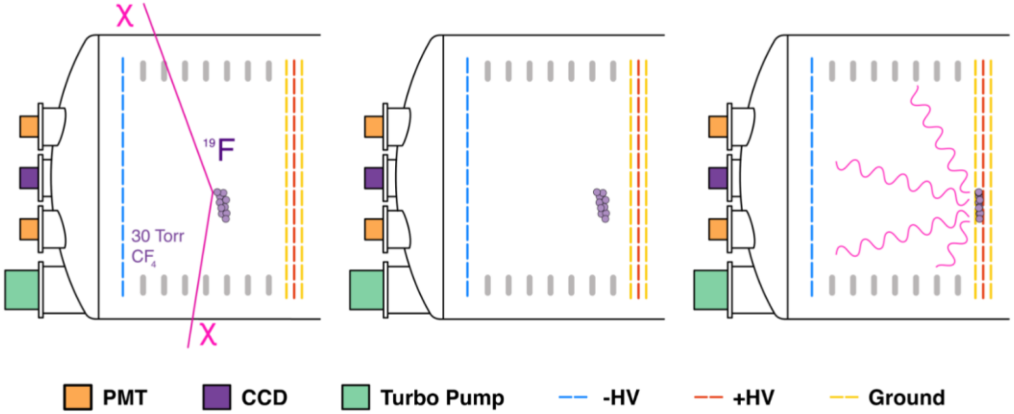

Subcomponents with different directions: boosted DM

Manty models predict boosted DM subcomponents

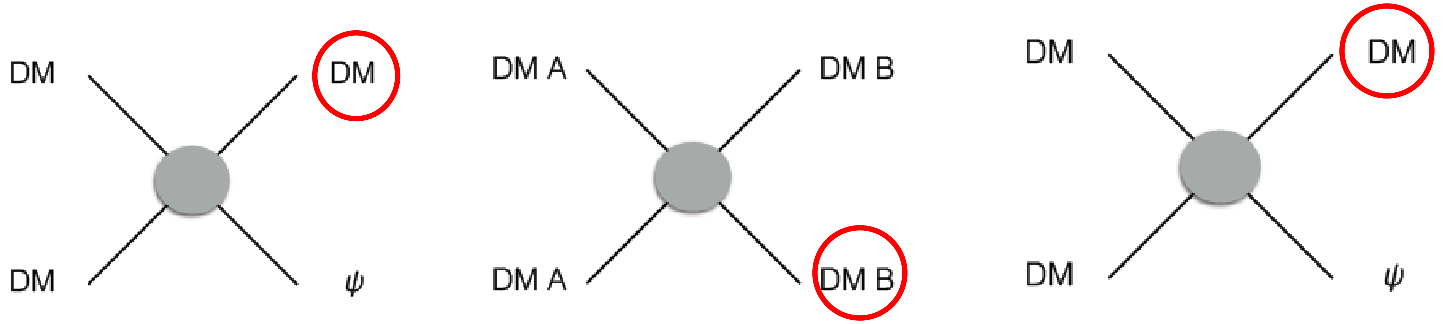

- Decay $A \to \bar{B}B$

$$\left(\frac{d\Phi_\chi}{dT_B d\Omega}\right)_{\rm dec} = \frac{1}{4\pi m_A \tau_A}\frac{dN}{dT_B}\int_{\rm l.o.s} d\ell \rho_\chi(\boldsymbol{r}),$$

- Annihilation $\bar{A}A \to \bar{B}B$

$$\left(\frac{d\Phi_\chi}{dT_B d\Omega}\right)_{\rm ann} = \frac{\langle\sigma_{\rm ann} v\rangle}{8\pi m_A^2}\frac{dN}{dT_B}\int_{\rm l.o.s} d\ell \rho_\chi^2(\boldsymbol{r}),$$

- 3→2 Semi-annihilation

$$\left(\frac{d\Phi_\chi}{dT_B d\Omega}\right)_{3\to 2} = \frac{\langle\sigma_{3\to 2} v^2\rangle}{24\pi m_A^3}\frac{dN}{dT_B}\int_{\rm l.o.s} d\ell \rho_\chi^3(\boldsymbol{r}),$$

J. Berger, Y. Cui, Y.Zhao. JCAP, (2015)

- Energy spectra well-determined
- Known angular distributions

DM boosted by astrophysical sources

- Sun (evaporation, reflection)

Kouvaris, et.tal 1506.04316, An, et.al, 1708.03642

- Blazar/AGN (up-scattering)

Wang , et.al, arXiv:2202.07598, arXiv:2202.07598

- Supernova (up-scattering)

Lin, et.al, arXiv:2206.06864

- Supernova remnants (up-scattering)

Cappiello et.al, arXiv:2210.09448

- Blackholes (Hawking evaporation)

Calabrese, et.al, arXiv:2107.13001
Chao, et.al, arXiv:2108.05608
Kitabayashi, arXiv.2204.07898

- Cosmic rays (up-scattering)

Bringmann, et.al, arXiv:1810.10543
Ema, et.al, arXiv: 1811.00520
Cappiello, et.al, 1arXiv:906.11283

CR-DM scattering:
an irreducible process for DM direct search

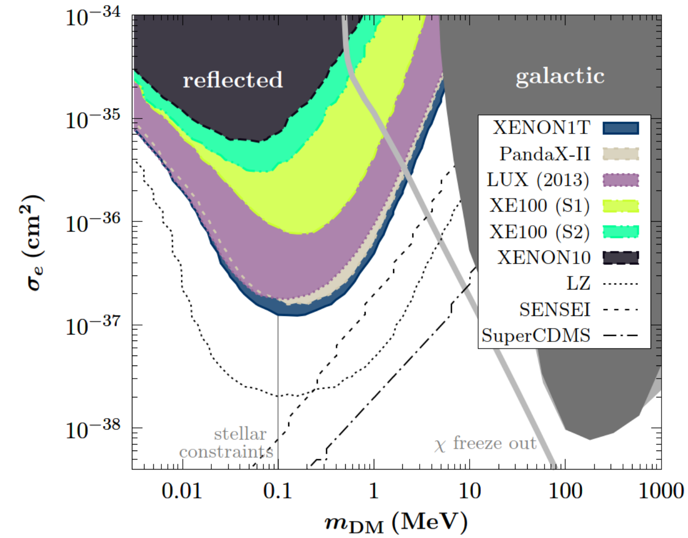

An, et.al, 1708.03642

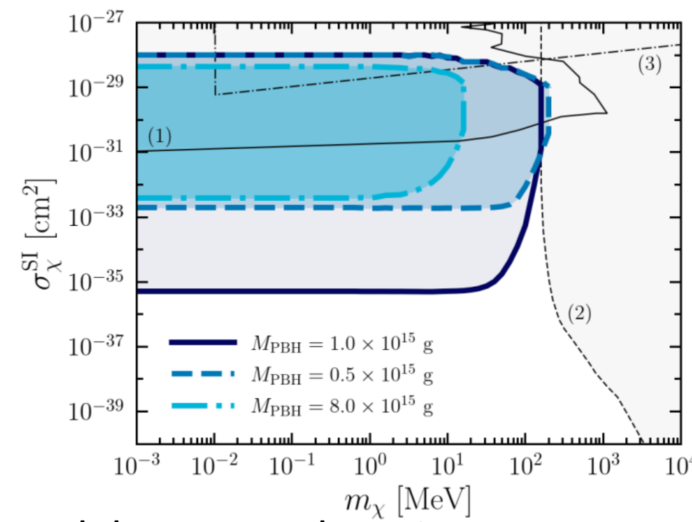

Calabrese, et.al, arXiv:2107.13001

CR-DM scattering: CR boosted dark matter

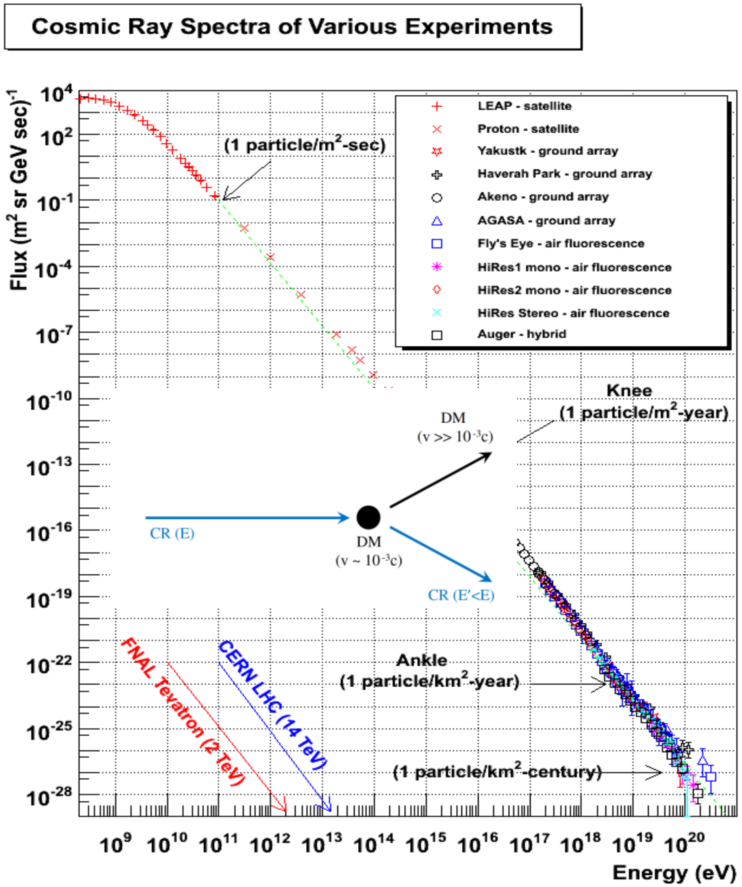

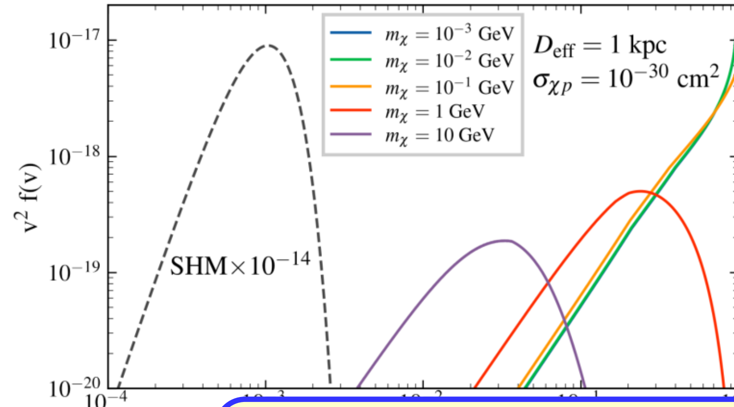

the most stringent limits set by neutrino detector

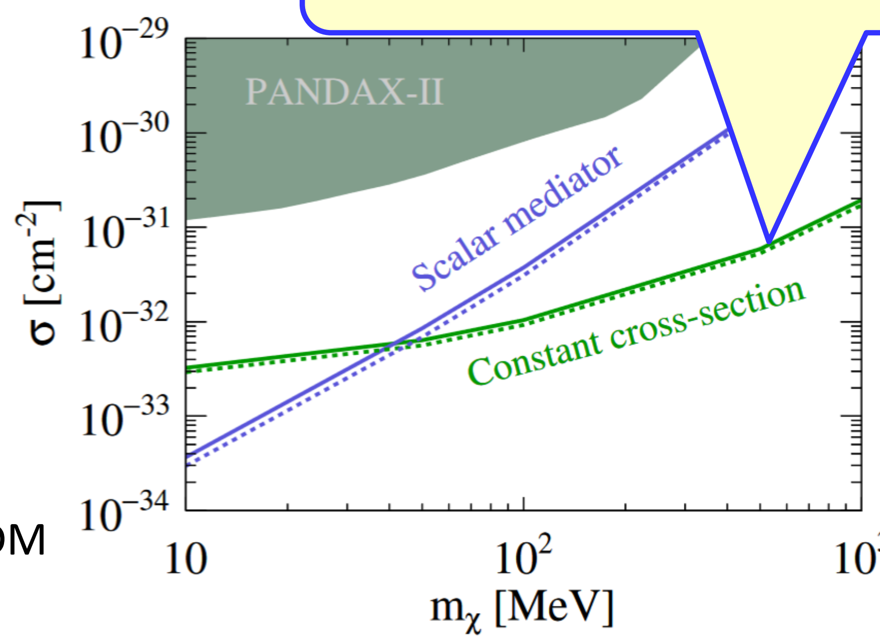

- Essentially no threshold problem
- Typical constraint $\sigma_{\chi p} < 10^{-(31-32)}\ cm^2$
- Constraints on $\sigma_{\chi N}$ highly insensitive to DM mass (for constant cross section)

The spectrum of CRDM

- DM flux from CR species *i*=proton, He, …

$$\frac{d\Phi_\chi}{dT_\chi} = \int_{l.o.s} d\ell \int_{T_i^{\min}}^{\infty} dT_i \left(\frac{\rho_\chi}{m_\chi}\right)\left(\frac{d\sigma_{\chi i}}{dT_i}\right)\left(\frac{d\Phi_i}{dT_i}\right)$$

drop rapidly towards higher E

enhancement factor

- A simplification: CR flux is similar to the locally measured one $\frac{d\Phi_i}{dT_i} \approx \frac{d\Phi_i^{LIS}}{dT_i}$
- The DM distribution can be factorized out (may not be accurate)

$$\frac{d\Phi_\chi}{dT_\chi} = \frac{\rho_\chi^{\rm loc} D_{\rm eff}}{m_\chi} \int_{T_i^{\min}}^{\infty} dT_i \left(\frac{d\sigma_{\chi i}}{dT_i}\right)\left(\frac{d\Phi_i^{\rm LIS}}{dT_i}\right)$$

with

$$D_{\rm eff} = \int_{l.o.s} d\ell \left(\frac{\rho_\chi}{\rho_\chi^{\rm loc}}\right)$$

DM distribution

CR local distribution

- Typical value of $D_{\rm eff}$ ~ a few kpc。

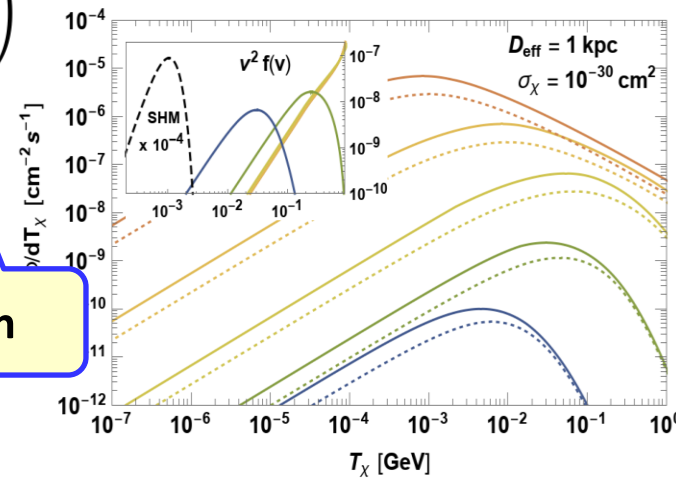

Bringmann, et al 1810.10543

morphological feature of the boosted DM flux

Distribution of DM flux close follows the sources

- DM boosted by the Sun, supervona, etc, point-like
- DM boosted by the dark sector diffuse, azimuthal symmetric
  - decay $$\left(\frac{d\Phi_\chi}{dT_B d\Omega}\right)_{\text{dec}} = \frac{1}{4\pi m_A \tau_A}\frac{dN}{dT_B}\int_{\text{l.o.s}} d\ell \rho_\chi(\boldsymbol{r}),$$
  - annihilation $$\left(\frac{d\Phi_\chi}{dT_B d\Omega}\right)_{\text{ann}} = \frac{\langle\sigma_{\text{ann}} v\rangle}{8\pi m_A^2}\frac{dN}{dT_B}\int_{\text{l.o.s}} d\ell \rho_\chi^2(\boldsymbol{r}),$$
  - $3 \to 2$ process $$\left(\frac{d\Phi_\chi}{dT_B d\Omega}\right)_{3\to 2} = \frac{\langle\sigma_{3\to 2} v^2\rangle}{24\pi m_A^3}\frac{dN}{dT_B}\int_{\text{l.o.s}} d\ell \rho_\chi^3(\boldsymbol{r}),$$
- DM boosted by CRs diffuse, **azimuthal asymmetric**

$$\frac{d\Phi_\chi}{dT_\chi d\Omega} = \int_{\text{l.o.s}} d\ell \frac{\rho_\chi(\boldsymbol{r})}{m_\chi}\int_{T_e^{\min}} dT_e \frac{\sigma_{\chi e}}{T_\chi^{\max}}\frac{d\Phi_e(\boldsymbol{r})}{dT_e},$$

Distribution of CR source

$$q(R,z) = \left(\frac{R}{R_\odot}\right)^a \exp\left(-b\frac{R-R_\odot}{R_\odot}\right)\exp\left(-\frac{|z|}{z_s}\right),$$

Diffusion halo $z_h \ll R_h$

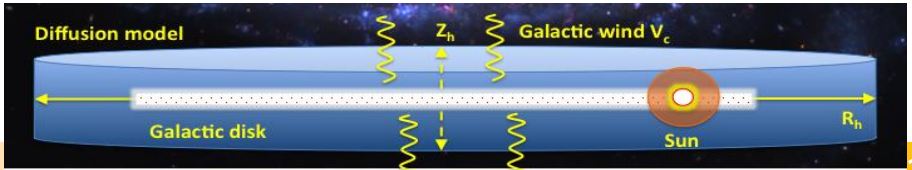

Azimuthal symmetry breaking in CRDM flux

Harmonic expansion

$$\frac{d\Phi_\chi}{d\Omega}(\theta,\varphi) = \sum_{l=0}^{\infty}\sum_{m=-l}^{l} a_{l,m} Y_{l,m}(\theta,\varphi),$$

coefficients

$$a_{l,m} = \int d\Omega Y^*_{l,m}(\theta,\varphi)\frac{d\Phi_\chi}{d\Omega}(\theta,\varphi).$$

- $a_{l,m}$ independent of $\sigma_{\chi e}$
- nonvanishing $a_{l,m}$ with $m \neq 0$ $\rightarrow$ azimuthal symmetry breaking

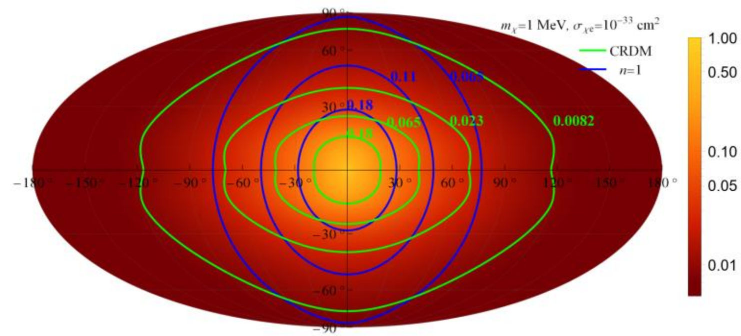

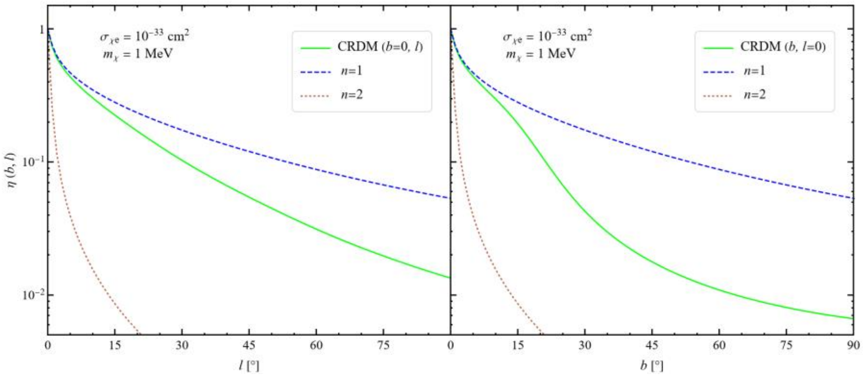

		$\tilde{a}_{1,0}$	$\tilde{a}_{2,0}$	$\tilde{a}_{3,0}$	$\tilde{a}_{4,0}$	$\tilde{a}_{5,0}$	$\tilde{a}_{2,2}$	$\tilde{a}_{3,2}$	$\tilde{a}_{4,2}$	$\tilde{a}_{4,4}$	$\tilde{a}_{5,2}$	$\tilde{a}_{5,4}$
NFW	CRDM	1.00	0.90	0.77	0.63	0.52	0.12	0.12	0.11	0.02	0.09	0.02
	BDM $(n=1)$	0.63	0.37	0.24	0.17	0.13	0	0	[illegible]	0	0	0
	BDM $(n=2)$	1.28	1.33	1.32	1.29	1.27	0	0	[illegible]	0	0	0
Einasto	CRDM	1.06	1.00	0.88	0.75	0.64	0.11	0.11	[illegible]	[illegible]	[illegible]	[illegible]
	BDM $(n=1)$	0.68	0.43	0.30	0.22	0.17	0	0	[illegible]	[illegible]	[illegible]	[illegible]
	BDM $(n=2)$	1.36	1.46	1.47	1.45	1.42	0	0	[illegible]	[illegible]	[illegible]	[illegible]

symmetry breaking term only appears in CRDM

Yan-Hao Xu, Chen Xia, YFZ, 2206.11454

Probing the morphology of CREDM flux

Cherenkov detectors can tell the arrival direction of DM

Detectors for neutrino experiments

1) Liquid scintillator detectors: Borexino, *Dune*

Low threshold (keV), no direction identification

2) Water Cherenkov detectors: *Super-K, SNO*

High threshold (MeV), can measure direction

3) Hybrid detectors, 1)+2): SNO+

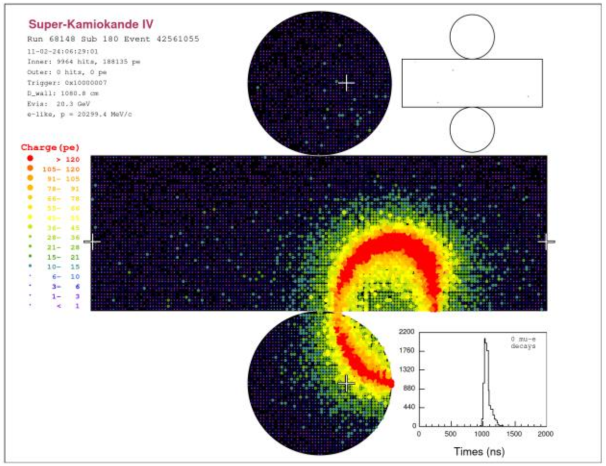

elastic electron scattering
Super-K (2018)

For boosted DM, the threshold is no longer a problem --> good news for neutrino experiments

- ❑ neutrino Exps. have huge exposures

e.g. SK: 50 kt

- ❑ Water Cherenkov detectors can measure direction

recoil electrons (and protons) following the direction of DM

SK has good angular resolution ~ 3°

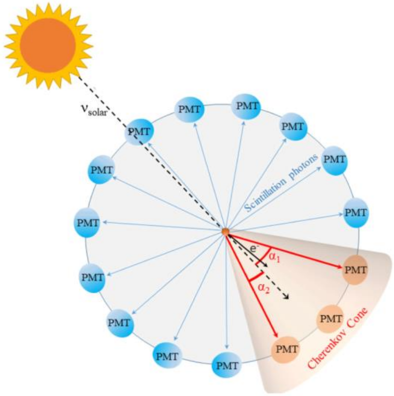

Borexino (2022)

Constraints on DM-electron scattering from SK-IV data

Optimize the search cone

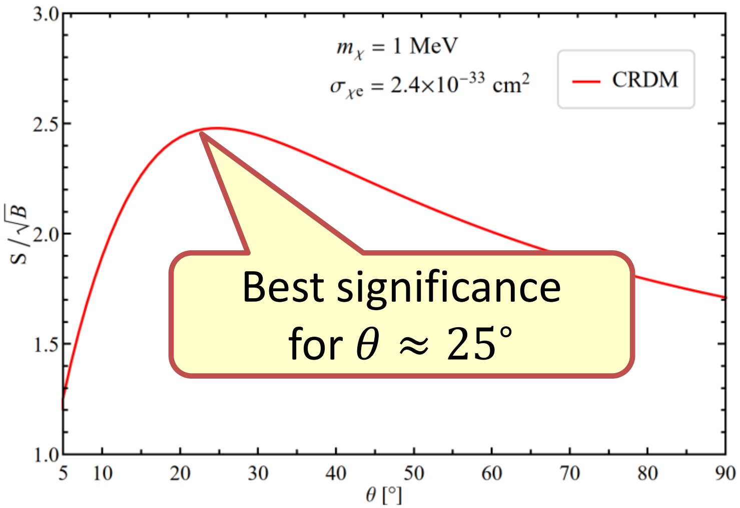

SK-IV all-sky data, 0.1–1.33 GeV

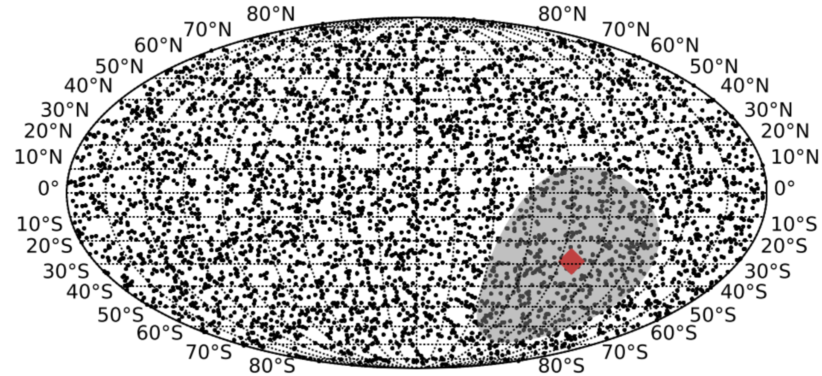

SK-IV background level: 1.96/kt/yr/sr

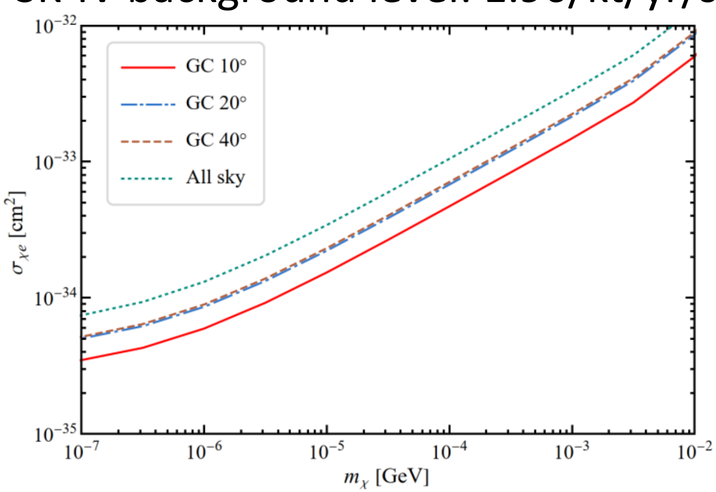

Limits at different cut-angles θ

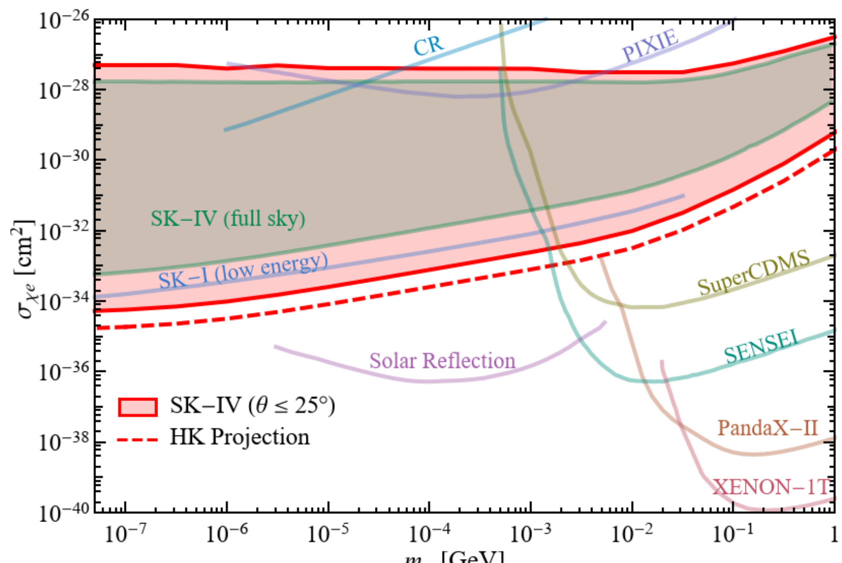

We obtain so far the most stringent limit
$\sigma_{\chi e} \leq 2.4 \times 10^{-33} cm^2 @1\ MeV$

Yan-Hao Xu, Chen Xia, YFZ, 2206.11454

Distinguishing CRDM from other boosted DM models

Define an azimuthal asymmetric parameter

$$A_R = \frac{N(\Omega_1) - N(\Omega_2)}{N(\Omega_1) + N(\Omega_2)},$$

Regions Ω_1 and Ω_2 are related by a 90^0 rotation

Optimize Ω_1/Ω_2 to maximize A_{R}

According to the SK background rate

future $A_{\mathrm{R}}^{HK} = 0.017 \pm 0.0055$

now $A_{\mathrm{R}}^{SK} = 0.017 \pm 0.036$

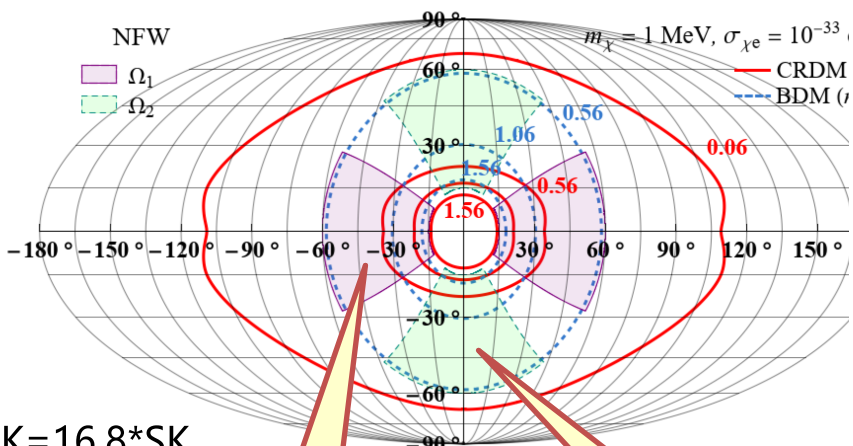

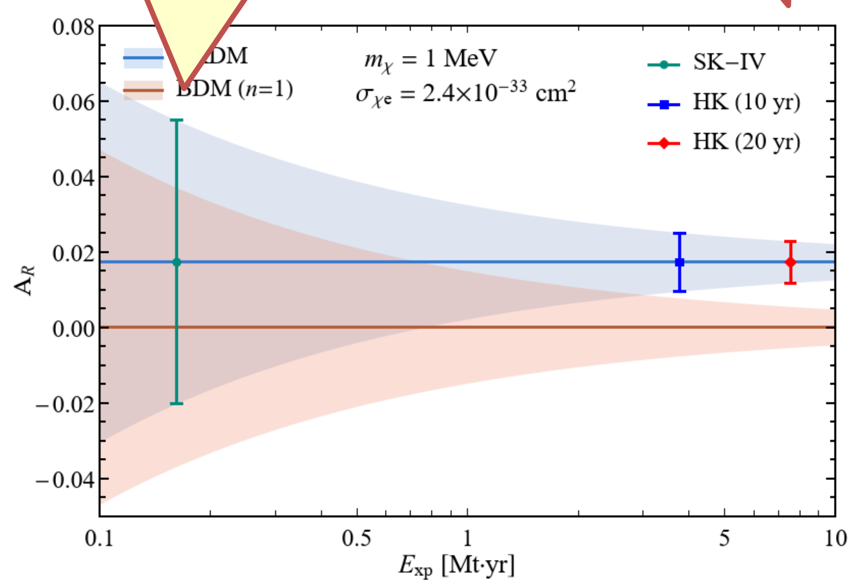

HK=16.8*SK

Ω_1

Ω_2

CRDM can be singled out from many boosted DM models

Yan-Hao Xu, Chen Xia, YFZ, 2206.11454 (PRD)

Indirect directional search: diurnal modulation

- **Annual modulation:** time-variation of halo DM flux
  - sensitive to halo DM (nonrelativistic)
  - apply to small cross section $\sigma_{\chi p} \sim O(10^{-40})$
  - modulation amplitudes typically small ($\leq 10\%$)

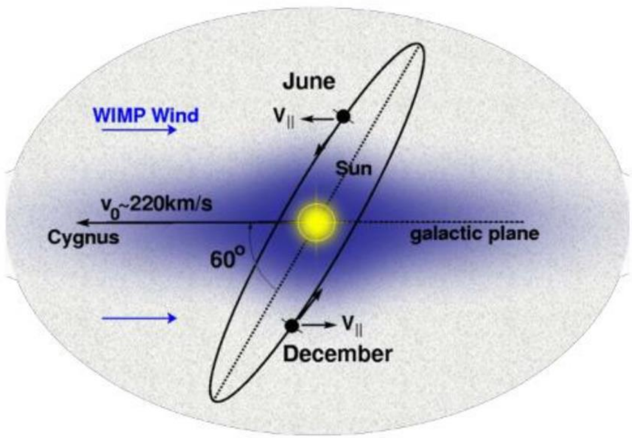

- **Diurnal modulation:** time-variation of relative position of the lab
  - sensitive to both halo DM and boosted DM
  - require large cross section $\sigma_{\chi p} \sim O(10^{-30})$
  - modulation amplitudes can be much larger

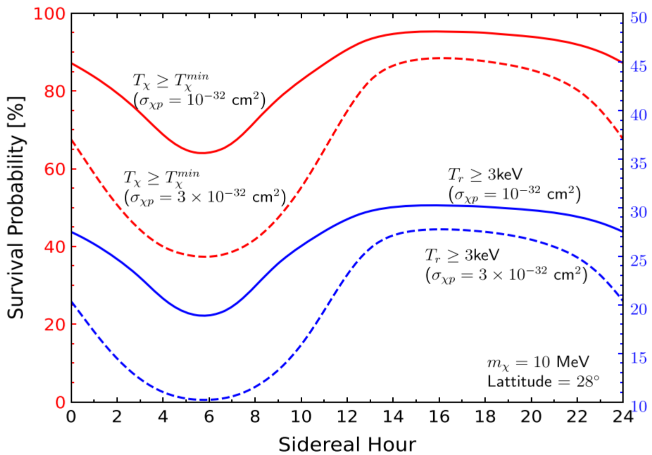

Ge, et al, arXiv:2005.09480 (PRL)

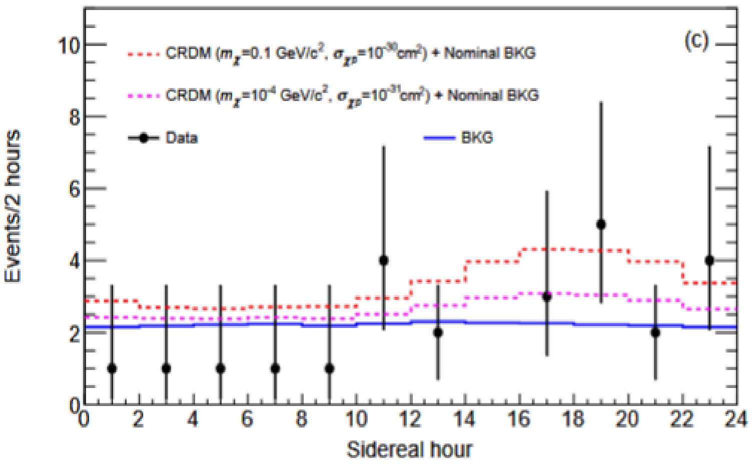

pandaX-II, arXiv:2112.08957 (PRL)

Diurnal modulation in electron recoil events ?

Current constraints on DM-electron scattering cross section are strong enough

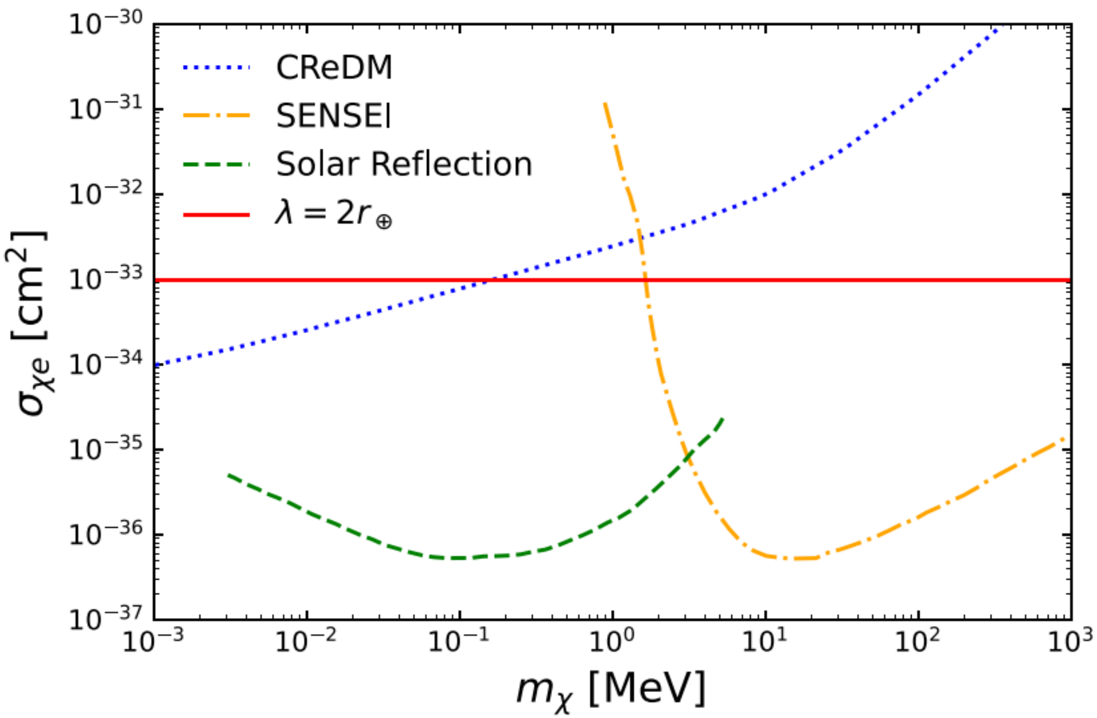

The DM mean-free-path is longer than the diameter of the Earth

Impossible to see diurnal modulation in electron recoil events ?

Electron signals from DM-nucleon scattering

- The Migdal effect

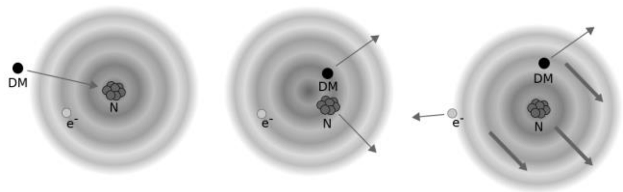

cross section

$$\frac{d\sigma_{\mathrm{Mig},nl}}{dT_N d\ln T_e} \approx \frac{1}{2\pi}\frac{d\sigma_{\chi N}}{dT_N}\frac{dP_{nl}}{d\ln T_e}(T_e,\, q_e)$$

Ionization probability

$$\frac{dP_{nl}}{d\ln T_e} \approx \frac{\pi}{2}\left|f_{nl}^{\mathrm{ion}}(k_e,\, q_e)\right|^2,$$

simple QM calculation

$$\left|f_{nl}^{\mathrm{ion}}(k_e,\, q_e)\right|^2 = \frac{2k_e}{\pi}\sum_{l'=0}^{\infty}\sum_{L=|l-l'|}^{l+l'}(2l'+1)(2l+1)(2L+1) \begin{pmatrix} l & l' & L \\ 0 & 0 & 0 \end{pmatrix}^2 \left|\int dr r^2 \widetilde{R}_{k_e l'}^{*} j_L(q_e r) R_{nl}\right|^2,$$

binding energies of the xenon atom

Orbital binding energy	$5p^6$	$5s^2$	$4d^{10}$	$4p^6$	$4s^2$	$3d^{10}$	$3p^6$	$3s^2$
RHF [eV]	12.4	25.7	75.6	163.5	213.8	710.7	958.4	1093.2
FAC [eV]	9.8	21	61	140	200	660	930	1100

energy spectrum of ionized electron (using FAC code)

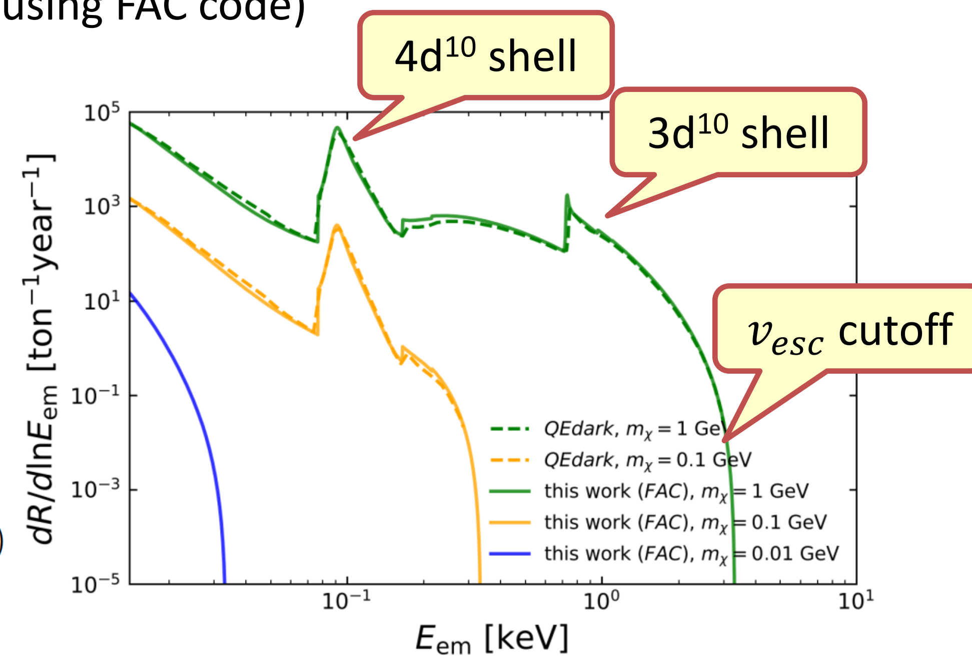

Underground DM flux and event rates

Underground DM flux can be higher

Mean energy-loss rate

$$\frac{dT_\chi}{dz} = -\sum_N n_N \int_0^{T_N^{\max}} \frac{d\sigma_{\chi N}}{dT_N} T_N dT_N,$$

But, assuming simple ballistic trajectories can be misleading

The numerical code (`darkprop`)

- ✓ anisotropic initial condition
- ✓ spherical Earth model with layers
- ✓ both relativistic and non-relativistic scatterings
- ✓ nuclear form factor
- ✓ fully cross-checked with `DaMasCUS`

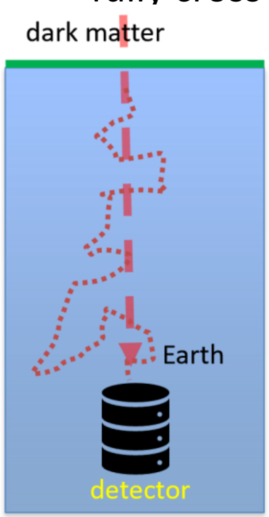

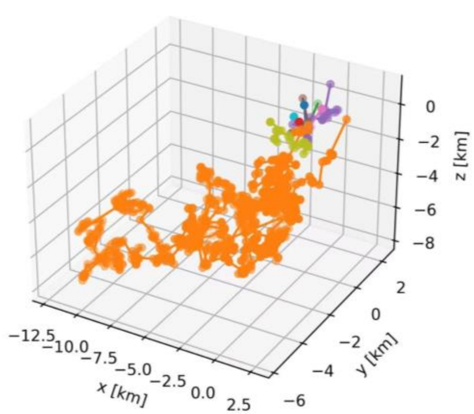

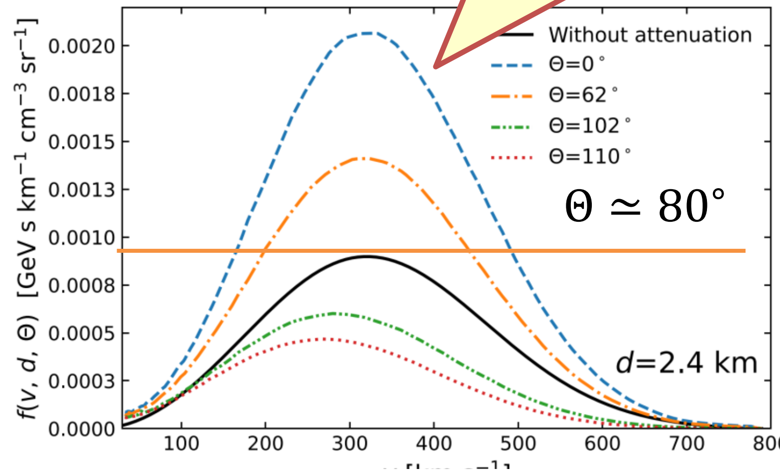

$$\frac{dR}{dE_{\rm em}} = \sum_{nl} \frac{1}{m_N} \int_0^\infty dT_N \int_{v_{\min}}^\infty dv \frac{d\sigma_{{\rm Mig},nl}}{dT_N dT_e} v f(v,\, d,\, \Theta)\,.$$

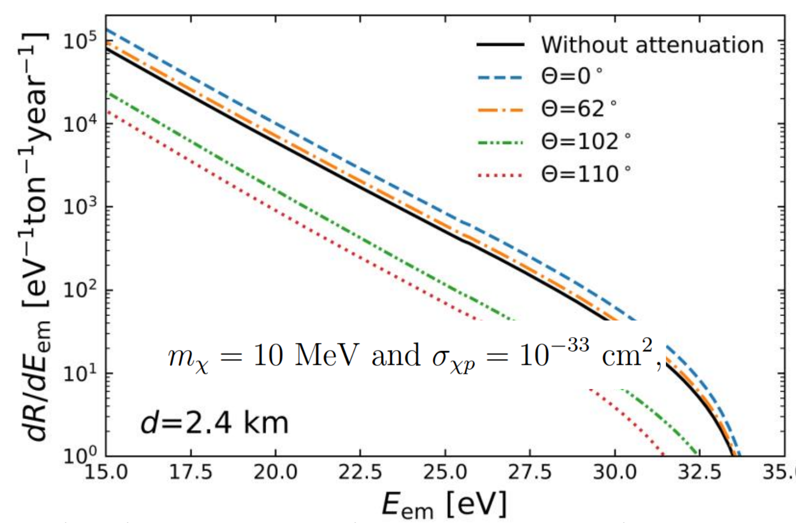

Mai Qiao, Chen Xia, YFZ , arXiv:2307.xxxx

Diurnal modulation amplitude

modulation amplitude

$$A(t) \equiv \frac{\int_{E_1}^{E_2} dE_{\rm em} \frac{dR(t,d)}{dE_{\rm em}}}{\frac{1}{T_\tau}\int_{t_0}^{t_0+T_\tau} dt R\left(t, d\right)}.$$

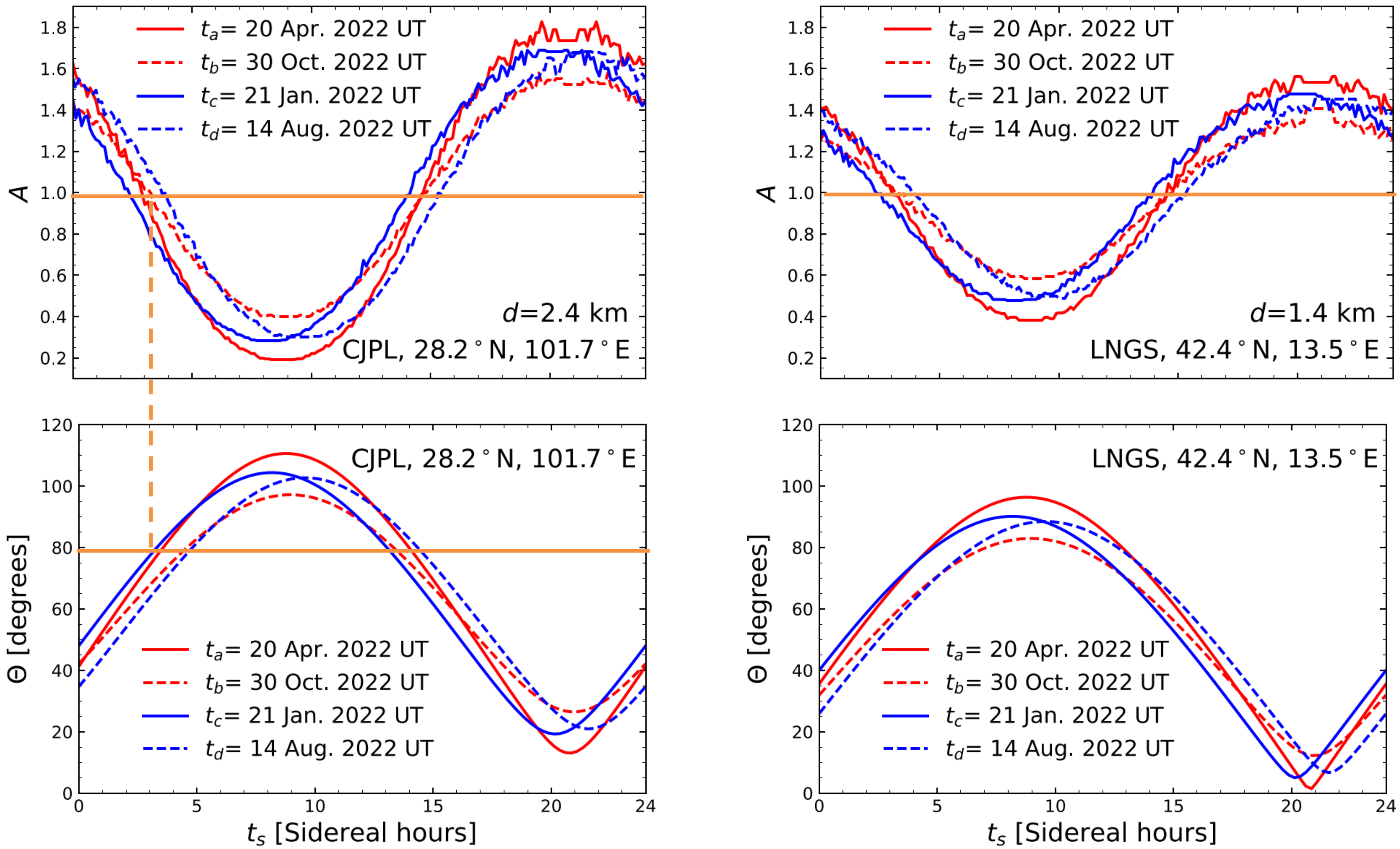

Limits form PandaX-II on the Migdal effect

binned Poisson method used to set limits at 90% C.L. from
PandaX-II (50-55 PE) , Xenon-10 (41-68 PE) and Xenon-1T (42-70 PE)

w/o Earth shielding

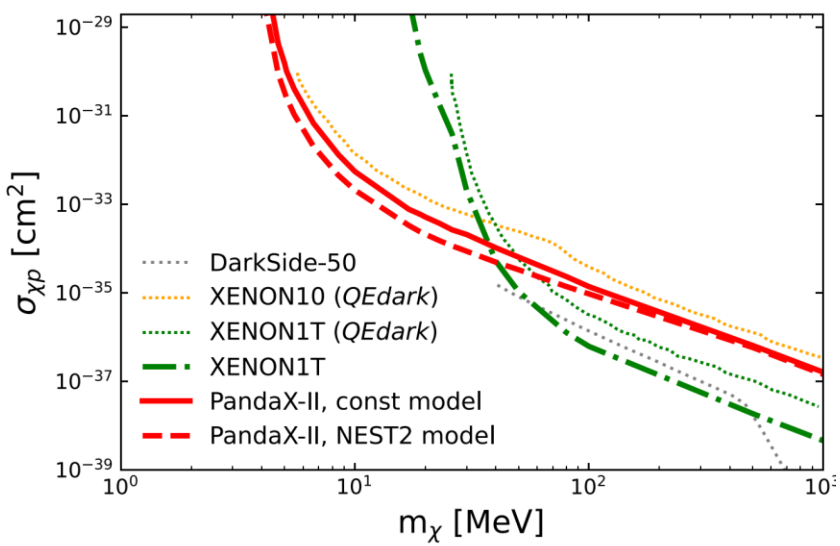

w/ Earth shielding

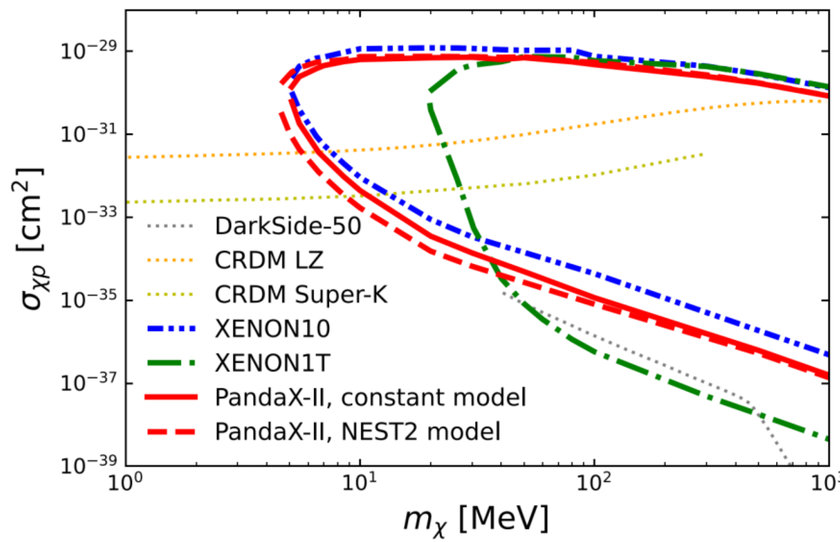

PandaX-II is leading the constraints on the Migdal effects !

Mai Qiao, Chen Xia, YFZ , arXiv:2307.xxxx

Predictions for diurnal asymmetry in electron events

Mai Qiao, Chen Xia, YFZ , arXiv:2307.xxxx

- Diurnal asymmetry for optimized two time bins

$$A_R = \frac{N(\delta t_{s,1}) - N(\delta t_{s,2})}{N(\delta t_{s,1}) + N(\delta t_{s,2})},$$

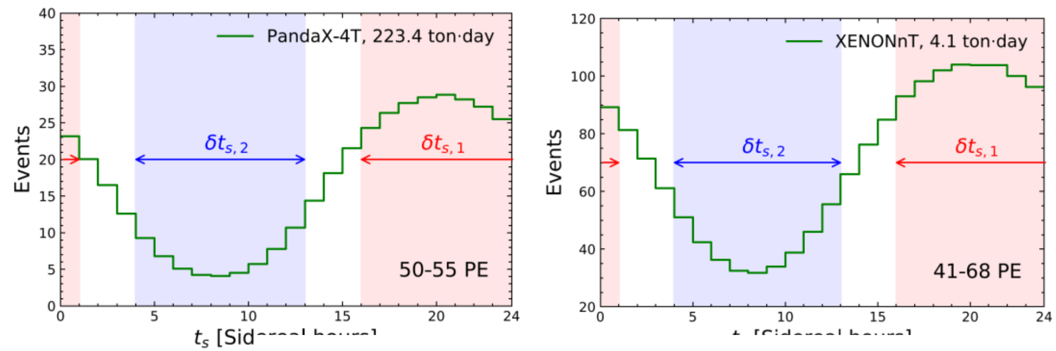

- Predictions for pandaX-4T and Xenon-nT $m_\chi = 10$ MeV and $\sigma_{\chi p} = 10^{-33}$ cm^2,

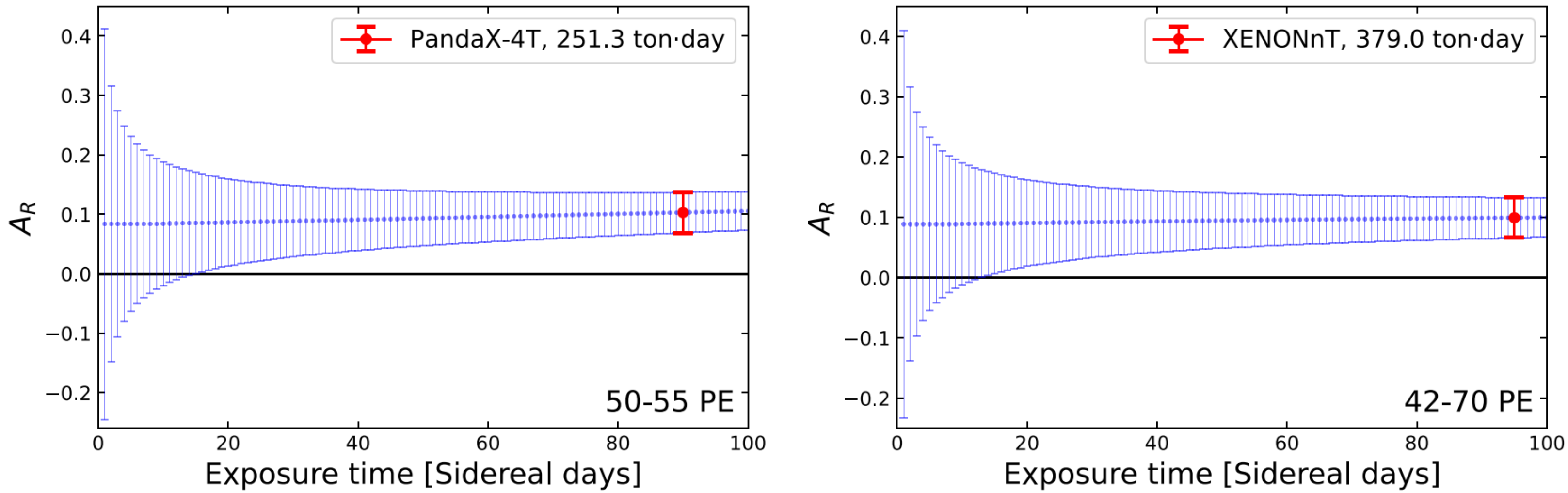

Summary

- In many models the DM flux observed on the Earth is anisotropic
- DM directional search (direct or indirect) are important to uniquely identify DM and distinguish different DM models.
- CRDM has unique morphological feature of azimuthal symmetry breaking, which can be used to improve the constraints, and distinguish it from many other boosted DM models at future neutrino experiment Hyper-K
- So far the most stringent constraints on Migdal effect is set by panaX-II. Observing the diurnal modulation of electron events from DM-nucleus scattering (Migdal effects) is promising, after consider all the current constraints

Backup slides

Effective exposures

Analysis	Exp Time	Fiducial Mass	Exp	Effective Exp	Eff Target Mass
XENON10 (14-203 PE) [1]	12.5 days	1.2 kg	15 kg·day	15 kg·day	1.2 kg
XENON1T [2]	278.8 days	1.3 ton	1 ton·yr	0.82 ton·yr	1.1 ton
XENON1T (150-3000 PE) [3]	258.2 days	0.39 ton (S2<400 PE)	100 ton·day	22 ton·day	85 kg
XENON1T (42-70 PE) [4]	7 days	0.39 ton	2.73 ton·day	12.7 kg·day	1.8 kg
PandaX-II [5]	401 days	0.329 ton	131.8 ton·day	131.8 ton·day	0.329 ton
PandaX-II (55-75 PE) [6]	400.9 days	0.117 ton	46.9 ton·day	46.9 ton·day	0.117 ton

TABLE I: Summation of the exposure time, fiducial mass, exposure and the effective target mass for different data analysis of XENON1T.

Background events

PandaX-II S2 bin [PE]	50-55	55-60	60-65	65-70	70-75
observed events	421	384	338	333	345
full exposure [ton · day]	131.8	131.8	131.8	131.8	131.8
effective exposure [ton · day]	46.9	46.9	46.9	46.9	46.9
background event rate [/ton/day] (rescaled by full exposure)	3.19	2.91	2.56	2.52	2.62
background event rate [/ton/day] (rescaled by effective exposure)	8.98	8.19	7.21	7.1	7.36

TABLE II: Summation of observed events and the assumed background event rate rescaled by the full exposure of 0.329 ton $\times$ 400.9 days and that rescaled by the effective exposure of 0.117 ton $\times$ 400.9 days, respectively, for PandaX-II.